IOP Publishing Quantum Sci. Technol. 8 (2023) 025003 https://doi.org/10.1088/2058-9565/acaf9d

Quantum Science and Technology

OPEN ACCESS

RECEIVED
7 April 2022

REVISED
25 October 2022

ACCEPTED FOR PUBLICATION
3 January 2023

PUBLISHED
23 January 2023

PAPER

Automatic generation of Grover quantum oracles for arbitrary data structures

Raphael Seidel*, Colin Kai-Uwe Becker, Sebastian Bock, Nikolay Tcholtchev, Ilie-Daniel Gheorghe-Pop and Manfred Hauswirth

Fraunhofer Institute for Open Communication Systems (FOKUS), Berlin, Germany
* Author to whom any correspondence should be addressed.

E-mail: raphael.seidel@fokus.fraunhofer.de

Keywords: quantum computing, oracle generation, Grover's algorithm, quantum logic synthesis

Abstract

The steadily growing research interest in quantum computing—together with the accompanying technological advances in the realization of quantum hardware—fuels the development of meaningful real-world applications, as well as implementations for well-known quantum algorithms. One of the most prominent examples till today is Grover's algorithm, which can be used for efficient search in unstructured databases. Quantum oracles that are frequently masked as black boxes play an important role in Grover's algorithm. Hence, the automatic generation of oracles is of paramount importance. Moreover, the automatic generation of the corresponding circuits for a Grover quantum oracle is deeply linked to the synthesis of reversible quantum logic, which—despite numerous advances in the field—still remains a challenge till today in terms of synthesizing efficient and scalable circuits for complex Boolean functions. In this paper, we present a flexible method for automatically encoding unstructured databases into oracles, which can then be efficiently searched with Grover's algorithm. Furthermore, we develop a tailor-made method for quantum logic synthesis, which vastly improves circuit complexity over other current approaches. Finally, we present another logic synthesis method that considers the requirements of scaling onto real world backends. We compare our method with other approaches through evaluating the oracle generation for random databases and analyzing the resulting circuit complexities using various metrics.

1. Introduction

1.1. General remarks

The field of quantum computing has seen a significant rise in interest over the past two years since the quantum supremacy announcement from Google [1] and will continue to be of great interest, among other things, due to the recent supremacy announcements regarding chinese quantum hardware designs [2–4]. Yet some of the well-known algorithms that are representative for the potential of quantum computing are still far from being implementable for meaningful applications on today's quantum hardware. Especially noteworthy are Shor's algorithm that could play a significant role in cryptography and cybersecurity as well as Grover's algorithm. The latter was initially designed for searching through large unstructured databases [5–7] but also has applications in cryptography [8] (e.g. for the search of encryption keys in the context of symmetric cryptographic algorithms), optimization problems [9–11]—that can even be beneficial for material discovery [12]—as well as applications for challenging problems in the domain of data structure and hash function design [13].

The focus of the research presented in this paper relates to the scalable synthesis of quantum oracles used in the context of Grover database search. The need for automatic oracle generation for Grover's algorithm was extensively discussed in one of our previous research works [14]. After a thorough analysis, [14] clearly states that there is a paramount requirement for automatically generated oracles as inputs for Grover's algorithm, in order to be able to provide function/procedure APIs (application programming interfaces) to developers and that way seamlessly integrate quantum computing into existing software development

projects (e.g. telecom supporting systems, web shops and other kinds of applications) and processes. In order to address this urgent need, we present the design and implementation of a fully automated programming framework for the complete Grover based search process, including the generation of the belonging quantum oracles. This involves the conversion of arbitrary data into Boolean functions that are encoded in truth tables, the synthesis of Grover oracles from these truth table expressions and the direct integration into the initialization and diffusion steps of Grover's algorithm.

1.2. Problem statement

The following constitutes a tangible list of aspects that summarize the targeted problem:

- The creation of oracles for Grover's search algorithm is a challenging task.
- The creation of quantum oracles containing the input for a Grover search needs to be done on a case-by-case basis depending on the database/list to search in and the object/value to search for.
- As of the current state-of-the art there is no accessible computer scientist's alike API for functions/procedures (e.g. *int grover(int [] list_to_search_in, int value_to_search_for)*) that allows for effortless submission of a database/list and an object/value to search for in this database/list.
- Hence, Grover's algorithm is almost impossible to apply for the execution of standard tasks in the course of programing IT components and products in different application domains.

In order to address the above issues, our current research paper presents a solution, such that efficient and convenient I/O procedures to Grover's algorithm are enabled. The following subsection outlines the specific contributions of our paper which address the posed problem statement and belonging research challenge.

1.3. Contributions

The following key contributions are the result of our research work, which is presented in the current paper toward progressing on the topic of automatic generation of Grover quantum oracles for arbitrary data structures:

(a) The current paper presents an overall structure of a procedure for the automatic generation of Grover oracles, which is based on truth tables and belonging quantum logic synthesis. This procedure enables Grover quantum search of arbitrary databases.
(b) We present a high level complexity analysis of this general structure/procedure and clearly identify the benefits and the need for improvements of the algorithms and the approach itself.
(c) Subsequently, we present a flexible method for implementing similarity searches over a database thereby steering the oracle generation correspondingly. Within a similarity search it is possible to utilize Grover's algorithm to identify database items which have a certain degree of resemblance compared to a particular item we are searching for.
(d) Moreover, we survey the topic of quantum logic synthesis and adapt different available algorithms—such as the *Reed–Muller Expansion* and the *Gray Synthesis* in order to improve their efficiency in the workflow of oracle generation.
(e) We present a new *Phase Tolerant Synthesis* method, a streamlined version of the established Gray Synthesis, which (asymptotically) halves the required resources.
(f) Another critical issue is constituted by the scaling of logic synthesis methods which quickly requires extremely fine phase gates. In order to address this issue we introduce the method of CSE-synthesis.
(g) Finally, we present a number of benchmarking results which confirm the efficiency of our approaches and algorithms for quantum logical synthesis and in general for automatic Grover oracle generation.

The above items constitute clear contributions, which to the author's knowledge are the first attempt so far to enable the efficient and convenient input of databases and objects to search for with Grover's algorithm with the goal to make it usable for different tasks in modern IT components and products (e.g. web portals, search engines, network operation centers, etc).

1.4. Structure of the paper

The rest of this paper is organized as follows: In section 2 we present an overview of the state-of-the-art in oracle synthesis work. In the subsequent section 3 our method for automatic oracles generation is presented. In section 4, we give an introduction into different methods for reversible quantum logic synthesis and elaborate on our improved version for Grover oracle generation that we denote as *phase tolerant synthesis*. This is then further discussed in the context of scalable logic synthesis circuit design in section 5. Section 6 describes the tests and results we obtained by comparing existing oracle generation methods with the one we

developed in terms of circuit complexity. Finally, section 7 contains a summary of the research presented in this paper as well as some brief discussion about our future research plans.

2. Overview and background

To provide an initial overview, section 2 reviews Grover's algorithm for efficient item search in unstructured databases on a higher level without going into the mathematical details and proofs. Afterwards, some recent research works from the domain of *Reversible Quantum Logic Synthesis* are presented. These activities and related results are of particular importance for our approach to the automated generation of Grover quantum oracles. Besides specific applications for Grover's algorithm, proof of concepts for experimental realizations [15] and low-scale prototype implementations on current quantum hardware [16], a really important field of research lies in the scalable generation of Grover oracles and quantum oracles for black box algorithms in general [14].

2.1. Grover's algorithm

At the heart of Grover's algorithm lies a quantum oracle, which phase-tags only the winner items. For now we leave the specifics of generating said oracle from the database to the subsequent sections and simply assume it has the following functionality:

$$O|i\rangle = (-1)^{f(i)}|i\rangle \text{ with } f(i) = \begin{cases} 0, & \text{if } i \notin \{w_j\} \\ 1, & \text{if } i \in \{w_j\}. \end{cases} \tag{1}$$

Note that for the oracle, we do not need to explicitly know w_j but we only need a valid function f for the search problem. Also for an explicit construction of such oracles, one generally needs an auxiliary qubit register to store intermediate results into which has to be uncomputed later on[1]. The role of this auxiliary qubit register and belonging operations is further discussed in section 3.

In order to evaluate Grover's algorithm with this oracle, we initialize the system in the fiducial state $|\Psi\rangle = |0\rangle^n$. Grover's algorithm starts by setting all qubits into an equal superposition state $|s\rangle$

$$H^{\otimes n}|0\rangle^n = \frac{1}{\sqrt{N}}\sum_{i=0}^{N-1}|i\rangle = |s\rangle. \tag{2}$$

Here, the integer states $|i\rangle$ directly relate to corresponding binary encoded states in the computational basis.

After phase-tagging the winner states—i.e. the states representing the values we search for in the unstructured database—Grover's algorithm implements a so-called diffusion operator $U_d = 2|s\rangle\langle s| - \mathbb{I}$ that amplifies the amplitudes for measuring the winner states. The phase-tagging and diffusion steps can geometrically be considered as two successively performed reflections, and thus as a single rotation in a 2D-plane. Each such rotation corresponds to a single Grover iteration that gradually rotates $|s\rangle$ closer to $|w_j\rangle$. At the end of the algorithm, a measurement in the computational basis is performed and the searched and potentially found items can be identified by distinct peaks in the distribution of the measured results. It is important to remark that in literature [17] there is a derived optimal number of Grover iterations (i.e. amplification and oracle application) that results in $|s\rangle$ being rotated the closest to $|w_j\rangle$. This optimal number of iterations yields the best measurement results. Thus, performing more or less rotations is expected to lead to increasingly worse search results. A more in-depth discussion about Grover iterations will be given in section 3. To summarize briefly: searching M items within an unstructured database needs at most $\mathcal{O}(\sqrt{\frac{N}{M}})$ iterations by Grover's algorithm. Hence there is a noticeable advantage over classical search algorithms, which are known to perform in $\mathcal{O}(N)$ for a linear search.

2.2. Reversible quantum logic synthesis

Technically, there is a deep interconnection between generating quantum oracles and synthesizing reversible quantum circuits from classical logic expressions. Therefore, in section 3 we describe the application of state-of-the-art quantum logic synthesis procedures for our approach to Grover oracle synthesis. In the following paragraph, we conduct a brief introduction to related research and development activities from the area.

As *Reversible Quantum Logic Synthesis* is an active field of research for more than 20 years [18], more efficient methods in terms of gate counts and the usage of ancilla qubits arise frequently [19]. While many of

[1] *Uncompation* is the process of *Garbage Collection* with respect to qubits, i.e. during an uncomputation the corresponding qubits are systematically reset to their initial states through the belonging reversible mathematical operations.

them are available in the *tweedledum* [20] library, a fairly recent method of interest is denoted as *resource-efficient oracle synthesis (ROS)* and was initially presented in [21]. It is built on the *LUT*[2]*-based hierarchical reversible logic synthesis framework* (LHRS) [22] and improves the LUT-network approach by adding a special quantum aware k-LUT mapper, involving specially truncated XAGs[3] and a more efficient SAT-based quantum garbage management technique[4] [23], which offers control over the number of qubits used in the synthesized circuits. This method can be considered as a reasonable competitor and thus constitutes an interesting research work for comparison to our synthesis methods. Additionally, there are some implementations for oracle generation in the established software frameworks like Qiskit [24] and Q# [25]. The Qiskit implementation will be tested and compared to our approach in section 6. Apart from the above mentioned activities, there are no further comparable methods to the best of our knowledge.

3. Method for automatic oracle generation

We will now present our method of turning arbitrary databases into oracles. The basic idea is to deploy a computationally effective labeling function, which turns the data into bitstrings of suited length. For a database D, this labeling will be denoted as[5]:

$$\begin{aligned} l : D &\to \mathbb{F}_2^k \\ e &\to l(e). \end{aligned} \tag{3}$$

Here, $k \in \mathbb{N}$ stands for the label size, which has to be chosen according to the specifics of the problem (more to that in section 3.1). The method of obtaining these bitstrings is in principle also free to choose as long as it only takes local information from the database, i.e. the bitstring of each element is independent from the rest of the database. For example, in our Python implementation, the native *hash* function generates an integer hash value for a wide class of objects, which we convert to the belonging binary representation and clip the bitstring to a length of k.

As a result, the labels provide a sequence of bitstrings representing the database, which eventually can be used to form a logical truth table (see figure 1(a) for an example). Subsequently, this truth table is turned into a quantum circuit using a suited quantum logic synthesis algorithm. Given two registers (the index and the label register) this yields a unitary mapping U_D which acts as:

$$U_D|i\rangle|0\rangle = |i\rangle|l(e(i))\rangle, \tag{4}$$

where $l(e(i))$ is the label of the database entry e with index i. It is important to note that the synthesis process only has to be done once per database. The resulting circuit can then be used for subsequent searches and only needs to be updated at changes to the database entries. We leave the challenge of efficient updating for database circuits as an open research question, which we are going to address in the near future.

Based on the above considerations, in order to **q**uery the index i_q for a given database element e_q, we combine the synthesized truth table with a phase-tag of the bitstring $l(e_q)$, which can be calculated with very small effort from e_q. The phase- tag is realized using a multi-controlled Z gate which is enclosed by X gates at the appropriate qubits. Finally, the label variable has to be uncomputed again. Denoting the tagging function of label $l(e)$ with $T(l(e))$, the mathematical description of the actions of the oracle $O(e_q) = U_D^\dagger T(l(e))U_D$ of the element e_q is as follows:

$$\begin{aligned} O(e_q)|i\rangle|0\rangle &= U_D^\dagger T(l(e_q))U_D|i\rangle|0\rangle \\ &= U_D^\dagger T(l(e_q))|i\rangle|l(e(i))\rangle \\ &= \begin{cases} -U_D^\dagger|i\rangle|l(e(i))\rangle & \text{if } l(e_q) = l(e(i)) \\ U_D^\dagger|i\rangle|l(e(i))\rangle & \text{else} \end{cases}, \\ &= \begin{cases} -|i\rangle|0\rangle & \text{if } l(e_q) = l(e(i)) \\ |i\rangle|0\rangle & \text{else} \end{cases} \end{aligned} \tag{5}$$

which is precisely the functionality we required $O(e_q)$ to have in equation (1).

[2] LUT stands for *lookup-table*.

[3] XAG stands for Xor-And-inverter Graphs, which constitute a particular form of representing intermediate results during the process of quantum logic synthesis.

[4] A management technique for the efficient uncomputation (i.e. garbage collection) of the corresponding circuits involving instances of the SAT-problem (SAT = SATISFIABILITY).

[5] $\mathbb{F}_2$ is the Galois field with two elements, i.e. the field of operation for traditional Boolean algebra. The arithmetic operations are all carried out $\bmod 2$, i.e. $1 + 1 \equiv 0 \bmod 2$. We will use the $\oplus$ notation for additions in the $\mathbb{F}_2$ space.

i	i_0	i_1	i_2	e	$l_0(e)$	$l_1(e)$	$l_2(e)$	$l_3(e)$
0	0	0	0	Alice	1	1	0	0
1	0	0	1	Bob	0	1	0	1
2	0	1	0	Craig	0	0	1	1
3	0	1	1	Dan	1	1	0	1
4	1	0	0	Eve	0	0	0	1
5	1	0	1	Faythe	0	0	1	0
6	1	1	0	Grace	0	1	0	1
7	1	1	1	Heidi	1	0	0	1

(a)

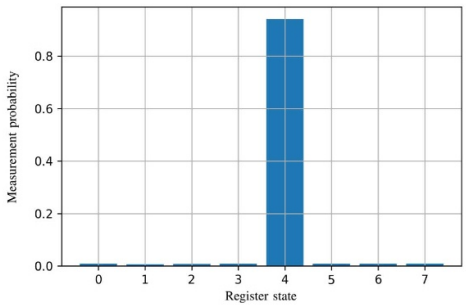

(b)

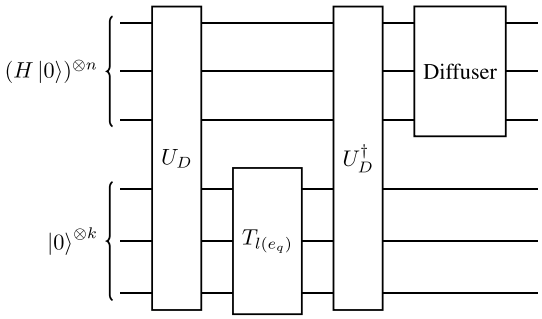

(c)

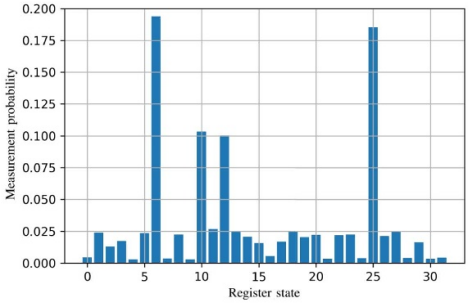

(d)

Figure 1. (a) Truth table of an example database containing some names as entries. The values for $l(e)$ are generated by truncating the binary strings from the output of Python's native *hash* function. (b) Example application of Grover's algorithm to the oracle created from the database in (a) querying for 'Eve'. The simulation was performed with *Qiskit*s OpenQASM simulator [26]. (c) Quantum circuit of a single Grover iteration querying for the database element $e_q \in D$. (d) Histogram of the measurement probabilities after applying Grover's algorithm to an oracle which uses the tagging gate from equation (10). As query label we used the label of the element at index 6 which is 110011. The label from index 10 is 010011 and the label at index 12 is 111011—both of these have Hamming distance 1 from the query label.

3.1. Hash collisions

As can be seen in figure 1(a), it can happen that two elements have the same label (here: Grace & Bob). This poses not that much of a problem, since after running Grover's algorithm a classical search can be applied on the (heavily reduced) result space. Another insight is constituted by the fact that the probability for a hash collision is well controlled by increasing/decreasing the label size (i.e. the size of the binary string). A second maybe more subtle problem is that in order to determine the optimal amount of Grover iterations R, the amount of tagged states has to be known according to [27]:

$$R \leqslant \left\lceil \frac{\pi}{4}\sqrt{\frac{N}{M}} \right\rceil \tag{6}$$

with M being the amount of elements sharing the labeling bitstring $l(e_q)$ and N the amount of elements contained in the database D. This might seem only like a minor inconvenience, because on first sight this could result in only a few extra-iterations. However, as described in the previous section, the results get worse if continuing with iterations after the optimal prescribed number. A possible quantum algorithm, which can determine M, is presented in [28]. Unfortunately, it requires exponentially many oracle calls, which is untenable for an efficient database and fast system reaction times. In addition, all these oracle calls have to be controlled, which implies that every CNOT gate is turned into a Toffoli gate[6] leading to another factor of 6 in the CNOT count. Due to these disadvantages, the approach is not feasible in practice, which is why we use a heuristic approach to estimate M. In detail, we determine the expected value of another element e_i colliding with the particular bitstring of e_0. For this we assume that the bitstrings are uniformly distributed over the label space $\mathbb{F}_2^k$. This is the setup for a Bernoulli-Process with $n = N-1$ tries with a probability of $p = 2^{-k}$. The resulting model is constituted by the binomial distribution and the expected value therefore takes the very simple form of:

$$\mathbb{E}(\#\text{collisions}) = np = (N-1)2^{-k}. \tag{7}$$

[6] A Toffoli gate is a controlled CNOT gate (or CCNOT). This gate can be synthesized using 6 CNOT gates.

Algorithm 1. Database encoder

```
Input: Iterable database D, labeling function
Output: Encoding circuit U_D
list bitstrings = []
for e in D do
    bitstrings.append(Label(e))
end for
TruthTable tt = TruthTable(bitstrings)
return QuantumLogicSynthesis(tt)
```

Since there is at least one element sharing the bitstring of e_0 (i.e. e_0 itself) we add a 1 to acquire the expected value for M:

$$\mathbb{E}(M) = 1 + (N-1)2^{-k}. \tag{8}$$

This formula captures the intuitive relationship between the label size k and the number of estimated hash collision M. It shows that by decreasing the label size k, one can increase M, while in parallel decreasing the amount of Grover iterations (see equation (6)) to be executed and synthesis tasks to be performed. This would be interesting in future hybrid use cases, where quantum resources are available at a similar cost as classical resources but still not capable of solving complex problems on their own. In this hybrid scenario, the search space would first be drastically lowered by a factor of $\mathcal{O}(2^{-k})$ by the quantum computer and then reduced to 1 with a classical search.

3.2. Algorithmic view on oracle generation

We want to continue by summarizing the overall procedure for the automated oracle generation from an algorithmic point of view. Thereby, we provide an overall structure of the steps which are required to generate an oracle for Grover's algorithm from a random database. These are structured in two sub-algorithms, namely the one responsible for database encoding (i.e. algorithm 1) and the second one, which is responsible for automatic definition of the oracle based on the encoded database (i.e. algorithm 2). Based on those two sub-algorithms, time complexity estimations are provided, in order to give a feeling regarding the applicability and the open research issues relating to the topic of automatic oracle generation.

Algorithm 1 describes the steps required to encode an arbitrary database for the purposes of Grover's search algorithm. The only requirement here is, that it should be possible to iterate over the content of the database. Thereby, no order of the content is presumed. Hence, the database can contain arbitrary objects.

The other ingredient, which is required as an input to algorithm 1, is the *labeling function*. This function needs to have the capability to take an arbitrary object from the database and assign it a label, that does not have to be unique. In fact, hash functions as known in computer science are natural choices as labeling functions. Hash functions in general do not provide unique labels (i.e. hash collisions). However, even with non-unique labels of the database objects, Grover search can be used to search for labels and that way reduce the overall search complexity by collapsing the search space only to those objects/entries, which have been assigned a particular label.

As can be seen in the listing of algorithm 1, a *for*-cycle is required that iterates over the database objects and assigns a label to each of them. This cycle has the time complexity of $\mathcal{O}(N)$, with N being the number of entries in the database. Each label is presumed to be a binary string and is stored in a corresponding list, which is used to initially prepare a truth table for Grover oracle. This truth table consists of simply listing and preparing the label bitstrings in such a way they can be used for quantum logic synthesis. Hence, the truth table creation has again complexity of $\mathcal{O}(N)$ and leaves the previous complexity estimation unchanged.

The quantum logic synthesis in the last step of algorithm 1 is the most critical part of the process. This step can be conducted by various algorithms and procedures, which is further focused on in the following sections of this paper, in which some fitting methods from literature are applied and evaluated and subsequently own methods are presented. As we will see in the upcoming section 4 this step can be performed quite efficiently using an algorithm called *Fast Hadamard–Walsh Transform* [29] which has classical time complexity $\mathcal{O}(N \times \log(N))$ per truth table column. In our case we synthesize about $k \approx \mathcal{O}(\log_2(N))$ in order to prevent excessive hash collisions, yielding an classical time complexity of $\mathcal{O}(N \times \log(N)^2)$.

However, as algorithm 1 has to be executed only once per fixed database, Grover's algorithm can be executed for different values to search for on the prepared database quantum circuit. Thus, the time complexity can be relieved this way with regard to the application of algorithm 1.

After the steps from algorithm 1 have been conducted, algorithm 2 must be executed every time before a new object/value is being searched for in the database entries. Algorithm 2 contains the required instructions

Algorithm 2. Query oracle generator

Input: Encoded database circuit U_D, query element e_q, labeling function
Output: Oracle circuit O
1: string qlabel = Label(e_q)
2: QuantumCircuit O = QuantumCircuit(index register, label register)
3: O.apply(U_D)
4: O.apply(PhaseTag(qlabel, label register))
5: O.apply($U_D^\dagger$)
6: **return** O

towards preparing a specific quantum oracle encoding the database and the search value. This specific quantum oracle is then embedded in Grover's algorithm for the subsequent search on the quantum computer side. We see the following components in algorithm 2: The creation of a *QuantumCircuit* object, in which the quantum circuit encoding the database (result from algorithm 1) is immediately embedded (i.e. O.apply(U_D) and finally O.apply($U_D^\dagger$) followed by the application of a phase tag (i.e. O.apply(PhaseTag (qlabel,labelregister))) for marking the value/object to search for. The steps in the first component are dominated by the embedding of the quantum encoded database circuit (i.e. O.apply(U_D) and finally O.apply($U_D^\dagger$) which can be considered linear with respect to the number of gates in the database quantum circuit. As we will see in the upcoming sections, the Gray synthesis method has a quantum gate complexity of $\mathcal{O}(N)$ per truth table column, implying a quantum gate complexity of $\mathcal{O}(N \times \log(N))$ for $k \approx \mathcal{O}(\log(N))$ columns. The phase tag (i.e. O.apply(PhaseTag(qlabel, labelregister))) and the diffuser can also be synthesized using Gray synthesis i.e. $\mathcal{O}(N)$. As we require $\mathcal{O}(\sqrt{N})$ Grover iterations, the overall quantum gate complexity is:

$$\mathcal{O}(N^{1.5} \times \log(N)). \tag{9}$$

On first sight this seems like a decrease in Grover's efficiency $\mathcal{O}(\sqrt{N})$ however we have to keep in mind that this is the complexity in *oracle calls* the oracle evaluation itself will have a non-constant complexity in almost any other comparable scenario.

Even though currently not more efficient than classical database search, our results open many research directions which could ultimately lead to an increase in database search efficiency.

Having briefly discussed this, the following sections continue with the presentation and deepen the discussion on various methods for quantum logic synthesis and for establishing Grover oracles and the search procedures in a flexible way.

3.3. Similarity search

The method presented so far can be generalized to a technique, which also allows for searching bitstrings *similar* to the query, i.e. not the exact item but rather one that is very close according to some metric. In the case, where the oracle has been generated from labeled data, this can obviously only work if the labeling function preserves the similarities between the database elements. Another application scenario for a *similarity search* could be the case where the labels themselves constitute the data.

The general idea of encoding the similarity of two bitstrings into the quantum oracle is to replace the tagging function $T^{\text{sim}}(l(e_q))$ with a circuit that performs phase shifts based on the Hamming-Distance. One such circuit is given by the application of RZ gates on the label register. In more detail:

$$T^{\text{sim}}(l(e_q)) = \bigotimes_{j=0}^{k-1} \text{RZ}_i \left(\frac{-(-1)^{l(e_q)_j} 2\pi}{k} \right). \tag{10}$$

For a single RZ gate acting on a qubit in a computational basis state we have:

$$RZ(-(-1)^x \phi)|y\rangle = \exp\left(\frac{i\phi}{2} (-1)^{x \oplus y} \right) |y\rangle. \tag{11}$$

Applying the similarity tag $T^{\text{sim}}(l(e_q))$ to the multi-qubit state $|l(e)\rangle$ therefore yields:

$$T^{\text{sim}}(l(e_q))|l(e)\rangle = \exp\left(\frac{i\pi}{k} \sum_{j=0}^{k-1} (-1)^{l_j(e_q) \oplus l_j(e)} \right) |l(e)\rangle. \tag{12}$$

To get an intuition of the effect of this, we now consider what happens when $l(e) = l(e_q)$. In this case we have:

$$l_i(e_q) \oplus l_i(e) = 0 \;\; \forall i < k, \tag{13}$$

implying that the sum over j evaluates to k. Therefore the applied phase is simply π, i.e. exactly what we have in the case of a regular phase-tag. If $l(e) = l(e_q)$ for all but one j-index, the sum evaluates to $k-2$. Hence, the applied phase is $\pi(1-\frac{2}{k})$ which is 'almost' the full phase-tag. An example application of the similarity search can be found in figure 1(d).

In the following, a more formal proof is presented regarding why the above considerations work when applied within Grover's algorithm. For this we assume that the oracle has tagged the uniform superposition $|s\rangle = \frac{1}{\sqrt{N}}\sum_{x=0}^{2^n-1}|x\rangle$ in such a way that the index register is in the state:

$$|\psi\rangle = \frac{1}{\sqrt{N}}\sum_{x=0}^{2^n-1}\exp(i\phi(x))|x\rangle. \tag{14}$$

We now apply the diffusion operator $U_s = 2|s\rangle\langle s| - \mathbb{I}$ on the above state:

$$U_s|\psi\rangle = \frac{1}{\sqrt{N}}(2|s\rangle\langle s| - \mathbb{I})\sum_{x=0}^{2^n-1}\exp(i\phi(x))|x\rangle = \frac{1}{\sqrt{N}}\sum_{x=0}^{2^n-1}\exp(i\phi(x))(2|s\rangle\langle s|\,x\rangle - |x\rangle). \tag{15}$$

Using $\langle s|\,x\rangle = \frac{1}{\sqrt{N}}$ gives:

$$= \frac{1}{\sqrt{N}}\left(\frac{2}{\sqrt{N}}\left(\sum_{x=0}^{2^n-1}\exp(i\phi(x))\right)|s\rangle - \sum_{x=0}^{2^n-1}\exp(i\phi(x))|x\rangle\right). \tag{16}$$

Next, we set

$$r_{\mathrm{cm}}\exp(i\phi_{\mathrm{cm}}) := \frac{1}{N}\sum_{x=0}^{2^n-1}\exp(i\phi(x)), \tag{17}$$

where cm stands for the center of mass. Inserting the definition of $|s\rangle$ we get:

$$\begin{aligned} &= \frac{1}{\sqrt{N}}\sum_{x=0}^{2^n-1}(2r_{\mathrm{cm}}\exp(i\phi_{\mathrm{cm}}) - \exp(i\phi(x)))|x\rangle \\ &= \frac{\exp(i\phi_{\mathrm{cm}})}{\sqrt{N}}\sum_{x=0}^{2^n-1}(2r_{\mathrm{cm}} + \exp(i(\phi(x) - \phi_{\mathrm{cm}} + \pi)))|x\rangle. \end{aligned} \tag{18}$$

Finally, we use the rules of polar coordinate addition:

$$r_3\exp(i\phi_3) = r_1\exp(i\phi_1) + r_2\exp(i\phi_2), \tag{19}$$

$$r_3 = \sqrt{r_1^2 + r_2^2 + 2r_1r_2\cos(\phi_1 - \phi_2)} \tag{20}$$

$$\phi_3 = \arctan\left(\frac{r_1\sin(\phi_1) + r_2\sin(\phi_2)}{r_1\cos(\phi_1) + r_2\cos(\phi_2)}\right), \tag{21}$$

to determine the absolute values of the coefficients in order to find out about the amplification factor A_x:

$$A_x = |2r_{\mathrm{cm}} + \exp(i(\phi(x) - \phi_{\mathrm{cm}} + \pi))| = \sqrt{1 + 4r_{\mathrm{cm}}^2 - 4r_{\mathrm{cm}}\cos(\phi(x) - \phi_{\mathrm{cm}})}. \tag{22}$$

From this we see that A_x becomes maximal if $\phi(x) - \phi_{\mathrm{cm}} = \pm\pi$, minimal if $\phi(x) - \phi_{\mathrm{cm}} = 0$ and is monotonically developing in between, which is precisely the behavior we expected.

Even though the similarity tag allows a considerable cut in the CNOT count compared to the multi-controlled Z gate, it comes with some drawbacks. The biggest problem is that the results of this method are very sensitive to the number of iterations. Applying the wrong amount of Grover iterations can lead to the case, where labels which are less similar get a higher measurement probability. This might be

improved through further analysis of the similarity phase-tags. Another drawback is that labels, where the bitwise NOT is similar to the query, get the same amplification as their inverted counter-part (assuming $\phi_{\text{cm}} = 0$ in equation (22)—more to this assumption soon). For example if we query for the label 000000, the label 011111 would receive the same amplification as 100000. This can be explained by looking at equation (12). If $l(e_q)$ and $l(e)$ differ on every single entry, we have:

$$l(e_q)_i \oplus l(e)_i = 1 \ \ \forall i < k. \tag{23}$$

This results in the sum evaluating to $-k$ and yielding a phase of $-\pi$, which is equivalent to a phase of π. A similar effect can be observed, when only a single bit of the inverse is mismatching. In this case, we apply the phase $-\pi + \frac{1}{k}$. Even though this phase is not equivalent to $\pi - \frac{1}{k}$, its absolute value is, which is the feature of relevance according to equation (22).

3.4. Advanced similarity tags

In this section we will present a method which lifts the restriction of the similarity tags being confined to the Hamming distance. Instead, it will be possible to encode an extremely wide and flexible class of similarity measures (without any overhead compared to the regular multi-controlled Z gate tags). If we denote the set of possible query objects with Q, any function with the following signature can be encoded as a similarity measure:

$$f\colon Q \times \mathbb{F}_2^k \to [0,1]. \tag{24}$$

Here $\mathbb{F}_2^k$ again denotes the set of bitstrings with length k and $[0,1]$ the interval between 0 and 1 (endpoints included). So this function compares a query object $q \in Q$ with a bitstring and returns a real number between 0 and 1, which indicates how similar the two objects are. 1 means equivalent and 0 means no similarity. An example of such a similarity measure is the Dice coefficient. In this case we have:

$$f\colon \mathbb{F}_2^k \times \mathbb{F}_2^k \to [0,1], \tag{25}$$

$$((x_0, x_1, \ldots, x_k), (y_0, y_1, \ldots, y_k)) \to \frac{2\sum_{i=0}^{k} x_i y_i}{\sum_{i=0}^{k}(x_i + y_i)}. \tag{26}$$

Note that the additions here are not denoted by $\oplus$ but the regular $+$ so they are not evaluated mod 2.

In order implement this advanced similarity tagging, we have to utilize the method of Gray synthesis which will be laid out in more detail in the coming section 4.2. All we need to know about it here is that it can synthesize arbitrary diagonal (in the computational basis) unitary matrices: For a given 2^k tuple of real numbers $\phi = (\phi_0, \phi_1, ..\phi_{2^k-1})$ a circuit $U_{\text{gray}}(\phi)$ can be synthesized such that for any computational basis state $|y\rangle$

$$U_{\text{gray}}(\phi)|y\rangle = \exp(i\phi_y)|y\rangle. \tag{27}$$

Note that Gray synthesis requires only up to 2^k CNOT gates, implying such a similarity tag is computationally more efficient or of equivalent efficiency as tagging with a multi-controlled Z gate.

We next show how applying Gray synthesis on the label register can be used to implement a tag, which acts as described in equation (14). Suppose we are given a similarity function f of the type in equation (24). Then the similarity tag $T_f^{\text{sim}}(q)$ for the query object $q \in Q$ is given as:

$$T_f^{\text{sim}}(q) = U_{\text{gray}}(\phi_f^{\text{sim}}(q)), \tag{28}$$

$$\text{where } \ (\phi_f^{\text{sim}}(q))_y = (-1)^y \pi f(q,y). \tag{29}$$

Next, we elucidate on the suitability of this operation as a similarity tag. For this we apply the similarity oracle consisting of the database encoding circuit[7] U_D and the similarity tag to the index register in a uniform superposition:

[7] Note that this circuit does not necessarily has to encode a database but any other function calculating a binary value is also possible. One such alternative use case are optimization problems, which is under active research by the authors. Because of this we write $U_D|x\rangle|0\rangle = |x\rangle|y(x)\rangle$ instead of the $l(e(i))$ language used in the previous sections.

$$\begin{aligned} O^{\text{sim}}(f,q,D)|s\rangle|0\rangle &= \sum_{x=0}^{2^n-1} U_D^\dagger T_f^{\text{sim}}(q) U_D|x\rangle|0\rangle \\ &= \sum_{x=0}^{2^n-1} U^\dagger T_f^{\text{sim}}(q)|x\rangle|y(x)\rangle \\ &= \sum_{x=0}^{2^n-1} U^\dagger \exp(i(-1)^{y(x)}\pi f(q,y(x)))\ |x\rangle|y(x)\rangle \\ &= \sum_{x=0}^{2^n-1} \exp(i(-1)^{y(x)}\pi f(q,y(x)))|x\rangle|0\rangle. \end{aligned} \tag{30}$$

We see that this oracle has the effect we assumed in equation (14) with $\phi(x) = (-1)^{y(x)}\pi f(q,y(x))$. First of all, we note that (under reasonable assumptions about f) the alternating signs of the phases help getting ϕ_{cm} close to zero. To see why this is the case, we assume that for the majority of $x < 2^n$, the statement $f(q,y(x)) < 0.5$ holds or in other words: Only in a few cases we actually do have similarity. Looking at the definition of ϕ_{cm} equation (17), we observe the repeated addition of complex numbers mostly in the right half of the complex plane, which implies that the center of mass is most likely going to be in the right half of the complex plane. As the signs of the phases are alternating, we 'balance' out the complex part by adding conjugates and non-conjugates which then implies $\phi_{\text{cm}} \approx 0$. If we now look at equation (22), we see that the relation between the similarity measure $f(q,y(x))$ and the amplification factor A_x is monotonical, which results in the desired behavior. Note that this does not imply that the amplification factor of x is proportional to the value of f. Only the ordering is preserved, i.e.

$$\text{if } f(q,y(x_1)) < f(q,y(x_2)) \tag{31}$$

$$\text{then } A_{x_1} < A_{x_2}. \tag{32}$$

An example application of Grover's algorithm to a similarity oracle implementing the Dice coefficient can be found in figure 2(a), where the above described aspects are clearly visible.

3.5. Contrast functions

Since we are only interested in the ordering of the values of the similarity measure, we can improve some properties without changing information by applying a monotonically increasing function with signature

$$\Lambda : [0,1] \to [0,1]. \tag{33}$$

We call this a *contrast function*. In other words: For a given similarity measure f and a contrast function Λ, instead of f we use $\tilde{f} = \Lambda \circ f$ as similarity measure (the $\circ$ denotes the composition[8]). An example of a contrast function which improved the results in many cases can be found in figure 2(d). Note that a large portion of the domain gets mapped to a value close to 0. This not only ensures the assumption $\tilde{f}(q,y(x)) < 0.5$ for most $x < 2^n$ (required for $\phi_{\text{cm}} \approx 0$) but also yields $r_{\text{cm}} \approx 1$ as in most cases $\phi(x) \approx 0$ (compare equation (17)). This in turn gives us a good amplification factor A_x for states that are supposed to be amplified but $A_x \approx 0$ for states that have only mediocre similarity (compare equation (22)).

4. Quantum logic synthesis

As pointed out in the previous sections, an integral part of generating oracles is the logic synthesis. There is a multitude of approaches each having their benefits and drawbacks. In this section, we focus on the *Reed–Muller Expansion* and *Gray Synthesis*. Subsequently, a new synthesis method developed by us is introduced, which is significantly more efficient in terms of general gate count. Our approach is to relax the constraint of all outputs having the same phase. This does not interfere with the outcome of Grover's algorithm as these phases cancel out during uncomputation. Finally, we derive and introduce another synthesis method, which addresses the pitfalls and requirements for scalable implementations of the belonging quantum circuits.

[8] For two functions g, h of fitting signature, the composition $g \circ h$ is the function which executes a successive application, i.e. $(g \circ h)(x) = g(h(x))$.

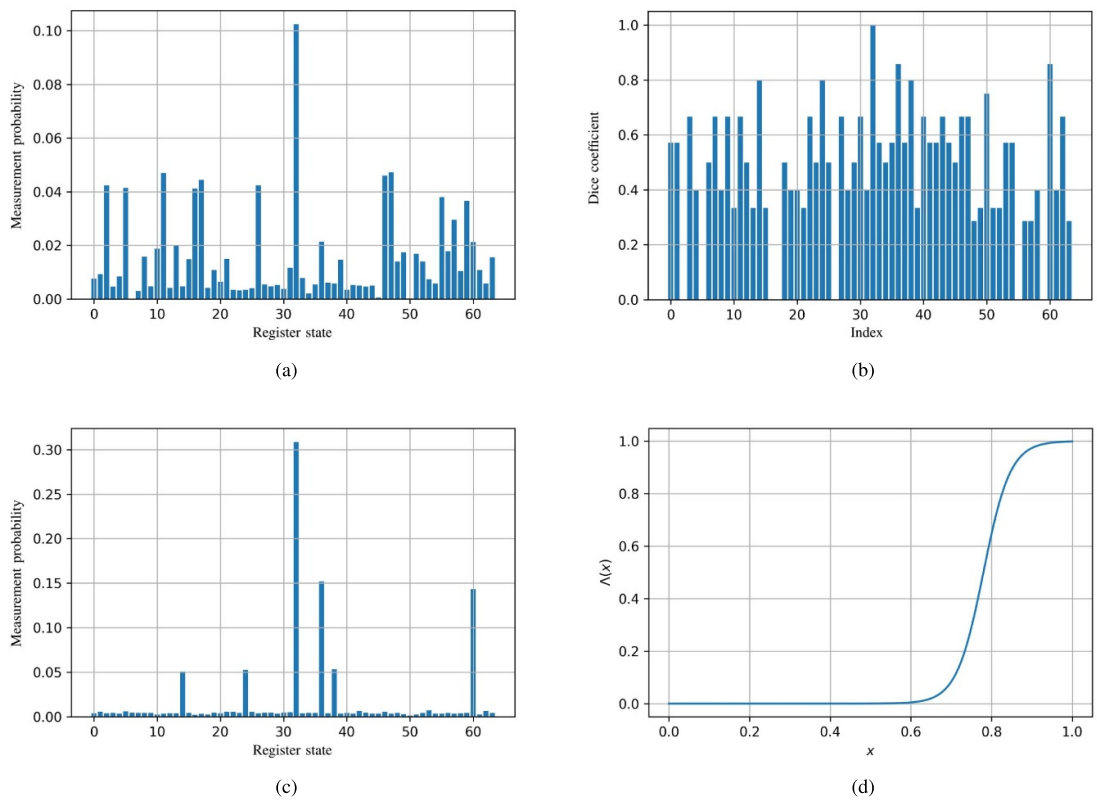

Figure 2. (a): Plot of the measurement probability of the index register after application of Grover's algorithm to a similarity oracle using the Dice coefficient as similarity measure of an example database of 64 entries. (b): The similarity measure (Dice coefficient) used in the oracle from (a). (c): The same plot as (a) but the similarity function has been wrapped in a contrast function. (d): The contrast function used in (c). The mathematical expression is $\Lambda(x) = (\exp(30(0.78 - x)) + 1)^{-1}$.

4.1. Reed–Muller expansion

The very first and foremost approach to tackle the challenge of logic synthesis is the Reed–Muller Expansion. Even though it is by far not the most efficient way to synthesize circuits for a quantum computer, it is basic concepts will be helpful for further understanding of the proposed concepts. The belonging method is denoted as positive polarity Reed–Muller expansion synthesis [30] and is abbreviated as PPRM accordingly for the rest of the paper.

First, we note that due to their reversible architecture, quantum computers do not have direct access to the full range of tools as in traditional logic synthesis. For example, we cannot infer the input constellation of a classical AND gate by just looking at the output. However, reversibility is a fundamental requirement to any quantum operation as there are only reversible building blocks available to construct said operation. But there is a way to turn any non-reversible gate into a reversible one which is keeping the inputs in place and saving the result into a new qubit. Using an n-controlled X gate we can therefore compute a multi-AND-gate between n-qubits into a new qubit. Acting with another (multi)-controlled X gate on the same qubit, we can realize an XOR gate. Expressions of the type:

$$(x_0 \text{ AND } x_1 \text{ AND } x_2) \text{ XOR } (x_0 \text{ AND } x_1), \tag{34}$$

are called XAG (**X**OR and **A**ND **G**raphs) and can be described very conveniently by polynomials over the Boolean algebra $\mathbb{F}_2$. The corresponding polynomial for equation (34) would be:

$$p(x) = x_0x_1x_2 \oplus x_0x_1. \tag{35}$$

Using this, we can introduce a very basic approach to quantum logic synthesis: Given a single column truth table T depending on n variables, its Reed–Muller expansion $RM_T^n(x)$ is the polynomial which is recursively generated by the following equation:

$$RM_T^n(x) = x_0 RM_{T_1}^{n-1}(x) \oplus (x_0 \oplus 1) RM_{T_0}^{n-1}(x), \tag{36}$$

Table 1. Example decomposition into co-factors. Note that while T is depending on two Boolean q variables, T_0 and T_1 are only depending on one variable.

x_0	x_1	T	T_0	T_1
0	0	0	0	—
0	1	1	1	—
1	0	1	—	1
1	1	1	—	1

here T_0, T_1 denote the co-factors of T, i.e. the truth tables considering the entries of T where $x_0 = 0$ or $x_0 = 1$ (see table 1). This recursion cancels at $n = 0$ with $RM^0_T(x)$ either equal to 0 or 1 depending on the value of $\tilde{T}$. The resulting polynomial is unique for any given truth table [31]. Given such a polynomial, one can generate the corresponding circuit implementation for a truth table by setting up a multi-controlled X gate for every 'summand' of the polynomial. While in principle sufficient, this method still has a lot of room for improvement as multi-controlled gates are computationally very expensive—[32] an n-controlled NOT gate requires $(2n^2 - 2n + 1)$ CNOT gates. For this reason, the following sections investigate further methods towards a more resource efficient synthesis of Boolean functions.

4.2. Gray synthesis

A more efficient synthesis method can be achieved by taking advantage of the non-classical properties of a quantum computer. This method is called Gray Synthesis and a detailed description is given in [33]. The method works with three types of gates: CNOT, H and T_m. While [33] also considers the possibility of directly synthesizing logic functions, these functions have to be $\mathbb{F}_2$-linear, which is an impermissible restriction in our case of application. In this paper, the focus on the possibility to synthesize a user-determined phaseshift for each computational basis state (now called 'input state'). This in turn can then be used to efficiently synthesize a truth table $T(x)$ by applying the method to the input register combined with the output qubit that is enclosed with H-gates. To illustrate how this works: consider that we synthesize a phase-shift of 0 for every input state that has a 0 in the output qubit and a phase-shift of $\pi T(x)$ for every state that has a 1 in the output qubit. This leads to the following calculation towards the synthesis of the desired truth table:

$$\begin{aligned} H_{\text{out}} U_{\text{gray}} H_{\text{out}} |x\rangle|0\rangle &= \frac{1}{\sqrt{2}} H_{\text{out}} U_{\text{gray}} |x\rangle(|0\rangle + |1\rangle) \\ &= \frac{1}{\sqrt{2}} H_{\text{out}} |x\rangle(|0\rangle + \exp(i\pi T(x))|1\rangle) \\ &= \frac{1}{\sqrt{2}} H_{\text{out}} |x\rangle(|0\rangle + (-1)^{T(x)}|1\rangle) \\ &= |x\rangle|T(x)\rangle. \end{aligned} \tag{37}$$

Here, the first ket $|x\rangle$ represents the input register, the second ket $|0\rangle$ the output qubit, and U_{gray} is the circuit which synthesizes the desired phases.

Since a good understanding of the phase synthesis method is a prerequisite to fully capture the power of phase tolerant synthesis, we will now go on to give a summary on how the phases are synthesized. A key concept in this context are parity operators, which basically are XOR expressions of different combinations of input variables e.g. $x_0 \oplus x_2 \oplus x_3$. Keep in mind, that we denote the XOR gates with the $\oplus$ symbol, because additions over real numbers will occur now too. The value of a parity operator on a given input state can be 'loaded' into a qubit by applying a sequence of CNOT gates (see figure 3(b) for an example). We can use the notion of parity networks to assign the desired phase to the input state by applying RZ gates onto the parity operators. Since RZ gates have the matrix representation $\text{diag}(\exp\left(\frac{-i\theta}{2}\right), \exp\left(\frac{i\theta}{2}\right))$, the change of phase $\Delta\phi$ after applying the gate $\text{RZ}(\theta_p)$ to a qubit, which has the parity operator p loaded can be written as:

$$\Delta\phi = \begin{cases} -\frac{\theta_p}{2} & \text{if } p(x) = 0 \\ +\frac{\theta_p}{2} & \text{if } p(x) = 1 \end{cases} = \frac{1}{2}(-1)^{p(x)}\theta_p, \tag{38}$$

the phase applied on a given input state $x = (x_0, x_1, ..x_n)$ after traversing the set of parity operators P can thus be summarized as:

$$\phi_x = \frac{1}{2}\sum_{p\in P}(-1)^{p(x)}\theta_p. \tag{39}$$

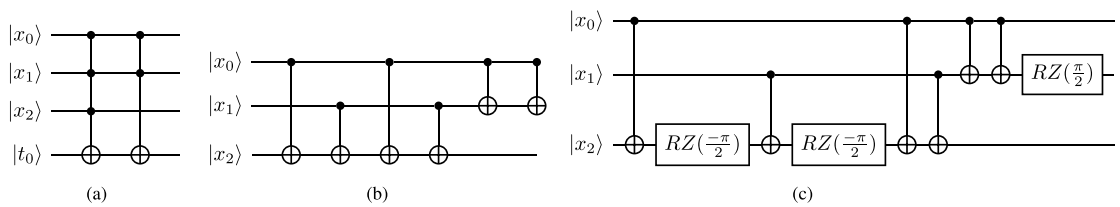

Figure 3. (a): Example synthesis of the polynomial in equation (34). (b): The corresponding circuit of the parity matrix given in equation (41). The sequence of parity operators traversed is $x_0 \oplus x_2, x_0 \oplus x_1 \oplus x_2, x_1 \oplus x_2, x_2, x_0 \oplus x_1, x_1, x_0, \emptyset$. (c): Example synthesis of $\phi = \pi(1,0,1,1,0,1,1,1,0)$. The solution of equation (40) is $\theta = \frac{\pi}{2}(-1,-1,0,0,0,1,0,2)$. The phenomenon of the last 2 CNOTs canceling out is treated in section 4.3.

Note that this is not a sum of $\mathbb{F}_2$ elements but of real numbers. We can therefore control what kind of phase each input state receives by carefully deciding on how to distribute the phase shifts θ_p. As each input state x can be uniquely identified[9] by just looking at the set of parity operators, which return 1 when applied to x, we can give each state a unique constellation of phase shifts by iterating over every possible parity operator. The next question is, how to determine the required $\theta = (\theta_{x_0}, \theta_{x_1}, \theta_{x_0 \oplus x_1} \ldots)$ phase shifts for a given sequence of desired overall phase shifts $\phi = (\phi_0, \phi_1, \ldots, \phi_{2^n})$? In this regard, by successively writing down, which state receives which phase shift one can set up a system of linear equations. The resulting matrix is denoted as the *parity matrix D*. The corresponding system of equations therefore yields:

$$\phi = \frac{1}{2} D\theta. \tag{40}$$

This is achieved by ordering the rows according to the natural order of the input states (i.e.000, 001, 010.) and the columns according to an algorithmic solution of the Hamming TSP[10], which visits all parity operators. The resulting matrix only depends on the number of input qubits. In the case of three input qubits we get:

$$D_3 = \begin{pmatrix} 1 & 1 & 1 & 1 & 1 & 1 & 1 & 1 \\ -1 & -1 & 1 & 1 & -1 & 1 & -1 & 1 \\ 1 & -1 & -1 & 1 & -1 & -1 & 1 & 1 \\ -1 & 1 & -1 & 1 & 1 & -1 & -1 & 1 \\ -1 & -1 & -1 & -1 & 1 & 1 & 1 & 1 \\ 1 & 1 & -1 & -1 & -1 & 1 & -1 & 1 \\ -1 & 1 & 1 & -1 & -1 & -1 & 1 & 1 \\ 1 & -1 & 1 & -1 & 1 & -1 & -1 & 1 \end{pmatrix} \tag{41}$$

Note that the last column corresponds to the 'empty' parity operator, which we define to be 0 on every input state. As the corresponding coefficient $\theta_\emptyset$ only induces an irrelevant global phase, it can be ignored during synthesis. Solving systems of linear equations is possible in $\mathcal{O}(N^3)$. Even though we only have to perform the synthesis once per database, this would still scale very bad compared to classical searching. A much more efficient solution is based on the following considerations: According to [21] the ith row of the Hadamard-Matrix H_N of degree N is the truth table of parity operator i. To be more precise the xth row of the ith column is equal to:

$$(H_N)_{xi} = (-1)^{i(x)}, \tag{42}$$

$$\text{where } i(x) = \bigoplus_{k=0}^{n-1} i_k x_k. \tag{43}$$

Since H_N is symmetric, this applies to the columns as well. Therefore our D is simply the Hadamard-Matrix with permuted columns, because this is precisely how the columns of D are defined:

$$H_N = D\Sigma, \tag{44}$$

[9] To see that this is true, consider two input states, where i is an index where the states differ. The parity operator x_i thus has differing values on the two states.

[10] The Hamming TSP stands for a TSP (traveling salesman problem) instance, where the Hamming distance is used as a distance measures between the involved entities/objects.

where Σ is some permutation matrix. We can now use a well-known property of H_N:

$$\begin{aligned} & H_N H_N^t = N\mathbb{I} \\ \Leftrightarrow\ & H_N^{-1} = \frac{H_N^t}{N} = \frac{H_N}{N}, \end{aligned} \tag{45}$$

to find the inverse of D:

$$\begin{aligned} D^{-1} &= (H_N \Sigma^{-1})^{-1} \\ &= \Sigma H_N^{-1} \\ &= \frac{\Sigma H_N}{N}. \end{aligned} \tag{46}$$

Applying this to equation (40), we get:

$$\theta = 2D^{-1}\phi = \frac{2\Sigma H_n \phi}{N}. \tag{47}$$

This can be interpreted as follows: θ is the Hadamard–Walsh transform[11] of ϕ up to some permutation and factor. Fortunately, H_n does not need to be explicitly calculated, since there is an algorithm called *Fast Hadamard Walsh Transformation* which performs the transformation in $\mathcal{O}(\log(N)N)$ [29].

4.3. Parity operator traversal

As the space of parity operators is the dual space for the vector space $\mathbb{F}_2^n$, it can be indexed by the natural numbers $< 2^n$. Finding a parity operator traversal route therefore reduces to finding a solution to an integer programming[12] traveling salesman problem [35]. The restricting feature here is, that we need one CNOT gate per bit that is changed in a traversal step. A possible solution for this is the Gray-Code [36]. The Gray-Code is a sequence of integers which traverse every single natural number $<2^n$ by only changing a single bit in every step. Even though it seems like this is precisely what is required, there is one drawback. As the Gray-Code traverses **every** parity operator, there is a considerable overhead, since only parity operators, which have a non-vanishing Hadamard-coefficient need to be traversed. This problem is addressed by a very simple heuristic solution. In order to ensure our traversal route ends where it started, we introduce a second salesman, which will meet the first after they both traversed the required integers. The resulting route will then be the route of the first salesman concatenated with the reversed route of the second salesman. Regarding the behavior of the individual salesmen, they always choose the closest parity operator, which has not been visited by either of them. We tried penalizing them for moving very far apart in order to reduce the reunification cost, which however did not lead to a significant reduction of the overall path length. Using this technique yields a (scale dependent) cut of about 10% in traversed parity operators, however it is significantly more expensive regarding the classical resources.

4.4. Phase tolerant synthesis

Even though Gray synthesis is already significantly cheaper in terms of CNOT gates than PPRM synthesis, there is an even bigger possible optimization with regard to the required quantum resources. During oracle application, we observe, that the label register always needs to be uncomputed after the winner state is tagged. This implies that we can be *tolerant* regarding the phases of the label variable as the tagging gate is not concerned with the involuntarily synthesized 'garbage phases'. To be more explicit, the synthesis methods discussed so far applied to an index register in uniform superposition would result in the state:

$$\sum_{x=0}^{2^n-1} |x\rangle |T(x)\rangle. \tag{48}$$

However a state like,

$$\sum_{x=0}^{2^n-1} \exp(i\chi_x)|x\rangle |T(x)\rangle, \tag{49}$$

[11] The Hadamard–Walsh transform [34] is closely related to Fourier analysis. It transforms complex numbers to a spectrum of orthogonal functions—these functions are called Walsh functions.

[12] The Hamming TSP and the integer/binary programming TSP are closely related, given that within the Hamming TSP we have binary strings as the entities and the Hamming distance as the distance between those entities. In this regard, the integer programming constitutes the problem formulation as a combinatorial problem with an optimization function over integers/bitstrings.

will be tagged in the correct way too and the 'garbage-phases' χ_x will be uncomputed, when the label register is uncomputed. In order to understand how to synthesize with garbage-phases, we note that in this method of synthesis, the logical information is only captured in the phase *differences* of the 0 and 1 state of the output qubit. Following the principles applied on equation (37), we arrive at:

$$\begin{aligned} H(\exp(i\phi_0)|0\rangle + \exp(i\phi_1)|1\rangle) &= \exp(i\phi_0)H(|0\rangle + \exp(i(\phi_1-\phi_0))|1\rangle) \\ &= \begin{cases} \exp(i\phi_0)|0\rangle \text{ if } \phi_1-\phi_0 = 0 \\ \exp(i\phi_0)|1\rangle \text{ if } \phi_1-\phi_0 = \pi. \end{cases} \end{aligned} \tag{50}$$

This observation can now be used in combination with a profitable choice of sequence of parity operators: Note how the parity network given in figure 3(b) visits every parity operator, which includes x_2 first and after that only operators which do not contain x_2. Furthermore directly after every parity operator which includes x_2 is visited, every circuit wire contains it is very own parity operator, i.e. wire 0 contains the parity operator x_0, wire 1 contains x_1 and so on. Therefore, we can simply end the synthesis procedure at this point, because every bit of phase that is synthesized after, does not differentiate between the $|0\rangle$ and the $|1\rangle$ state of the output qubit (which would be x_2 here), and therefore does not contribute anything to the phase difference of the $|0\rangle$ and the $|1\rangle$ state.

To make this notion accessible from a more formal point of view, consider the case that we are applying Gray synthesis to the state of uniform superposition $|s\rangle$:

$$|s\rangle = \frac{1}{\sqrt{2^n}} \sum_{x=0}^{2^n} |x\rangle. \tag{51}$$

We factor out the output qubit:

$$|s\rangle = \frac{1}{\sqrt{2^n}} \sum_{x=0}^{2^{n-1}} (|0\rangle + |1\rangle)|x\rangle. \tag{52}$$

The 'first step' in this view of Gray synthesis is synthesizing phases $\phi_{(0,x)}$ and $\phi_{(1,x)}$ on the output qubit:

$$U_{\text{gray}}^{\text{Step 1}}|s\rangle = \frac{1}{\sqrt{2^n}} \sum_{x=0}^{2^{n-1}} \left(\exp(i\phi_{(0,x)})|0\rangle + \exp(i\phi_{(1,x)})|1\rangle\right)|x\rangle =: |\psi\rangle. \tag{53}$$

The second step would now be to synthesize a phase on the remaining qubits which could be seen as 'correcting' the garbage phase χ_x. This however does not change the relative phase of the $|0\rangle$ and $|1\rangle$ state of the output qubit:

$$U_{\text{gray}}^{\text{Step 2}}|\psi\rangle = \frac{1}{\sqrt{2^n}} \sum_{x=0}^{2^{n-1}} \exp(-i\chi_x)\left(\exp(i\phi_{(0,x)})|0\rangle + \exp(i\phi_{(1,x)})|1\rangle\right)|x\rangle. \tag{54}$$

The important point of phase tolerant synthesis is that the *difference* $\phi_{(0,x)} - \phi_{(1,x)}$ determines the result of the logic output state:

$$\phi_{(0,x)} - \phi_{(1,x)} = \begin{cases} 0 & \text{if } T(x) = 0 \\ \pi & \text{if } T(x) = 1. \end{cases} \tag{55}$$

Note that while we in principle could determine the phases $\chi_x, \phi_{(0,x)}, \phi_{(1,x)}$ from the user specified input phases $(\phi_0, \phi_1 .. \phi_{2^n})$, it is neither necessary nor relevant. Just breaking the routine after the first step equation (53) was performed, is sufficient. For an example check figure 4.

5. CSE synthesis

In this section, we present further progress beyond state-of-the-art from our research activities—the implementation of quantum logic synthesis under the consideration of restrictions in a real world setup. Phase tolerant Gray synthesis may be very resource friendly to both classical and quantum resources, however scaling on real devices is still challenging: Taking a look at equation (47) we see that, because the only values of the entries of ϕ that can appear in the scenario of logic synthesis are $\pm\frac{\pi}{2}$. Therefore the values of the entries of ϕ are integer multiples of $\pm\frac{\pi}{N}$. This implies that if we want to encode an array with N entries,

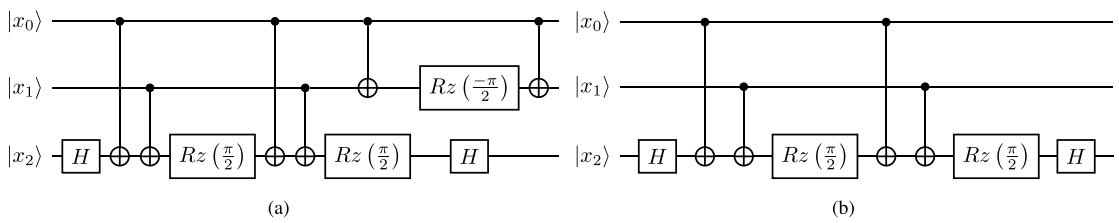

Figure 4. (a) Logic synthesis of the two input-bit truth table 1001. (b) Phase tolerant logic synthesis of the two input-bit truth table 1001. Note that we only need to use four instead of six CNOT gates. The savings converge to 50% for larger truth tables.

we will need reliant $\frac{\pi}{N}$ RZ gates[13] are. As this quantity will be central in the upcoming discussion, we will refer to the *T-order* of a circuit by the minimal number $m \in \mathbb{N}$, such that every phase gate can be expressed as an integer multiple of a $\frac{\pi}{2^m}$ phase gate[14].

Another ineffectiveness we observe is the fact that there is no usage of redundancy for the synthesis of multiple truth table columns even though we know that we will synthesize about $\mathcal{O}(\log(N))$ columns. In the worst case we have the same column twice which means two syntheses procedures, although one synthesis + 1 CNOT gate would be sufficient. This handmade solution requires about half the resources, raising the question for an automatization of this procedure.

Both of these problems can be tackled by an approach based on calculating intermediate results and intelligently optimizing the next synthesis steps accordingly. Such an approach has already been proposed in [21]. Even though the authors could effectively demonstrate a reduction in the T-order, their technique still does not consider redundancies, since they focus on synthesizing truth tables with only a single column. Even though very heavy on the classical resources side and moderate on the qubit count, our approach (presented in this paper) has been shown to significantly reduce the T-order (see table 3). The basic idea lies in automated algebraic simplifications. As we saw in section 4.1, a single column truth-table can be represented by a $\mathbb{F}_2$-polynomial. Multi-column truth tables can be therefore be interpreted as tuples of $\mathbb{F}_2$ polynomials $f(x) = (f_1(x), ..f_n(x))$. The key step is now to apply the common sub-expression elimination (CSE) algorithm of the computer algebra system (CAS) library *sympy*[15] to these polynomials. This will give a sequence of intermediate values which reduce the overall resources required for the evaluation of f. For example, given the truth table:

x_0	x_1	x_2	f_0	f_1	f_2
0	0	0	0	1	0
0	0	1	1	0	0
0	1	0	1	0	0
0	1	1	0	1	0
1	0	0	1	1	0
1	0	1	1	0	0
1	1	0	0	0	0
1	1	1	0	1	1

by applying Reed–Muller Expansion we get:

$$f_0(x) = x_0x_2 \oplus x_0 \oplus x_1 \oplus x_2 \tag{56a}$$

$$f_1(x) = x_0x_1 \oplus x_0x_2 \oplus x_1 \oplus x_2 \oplus 1 \tag{56b}$$

$$f_2(x) = x_0x_1x_2. \tag{56c}$$

[13] According to [37] it is possible to implement RZ gates virtually without any error and duration, however this might not be the case for every physical qubit realization.

[14] According to [38] a logical qubit of a circuit of order m in fault tolerant implementation (using the punctured Reed–Muller Code) requires (up to) $2^{m+2} - 1$ physical qubits.

[15] SymPy CAS: www.sympy.org, as of 3 August 2021.

We now apply the CSE algorithm, which yields two intermediate values g_0 and g_1:

$$g_0(x) = x_0x_2 \tag{57a}$$

$$g_1(x) = g_0(x) \oplus x_1 \oplus x_2. \tag{57b}$$

The results utilizing the intermediate values are now:

$$f_0(x) = g_1(x) \oplus x_0 \tag{58a}$$

$$f_1(x) = g_1(x) \oplus x_0x_1 \oplus 1 \tag{58b}$$

$$f_2(x) = g_0(x)x_1. \tag{58c}$$

Note that a product of k variables will give a k-controlled X gate in PPRM synthesis[16]. Synthesizing such a gate is equivalent to a truth table with 2^m entries, which implies that the T-order for a circuit containing only m-products or lower is m. Note that the synthesis of equation (56c) contains a product of three variables, which implies that it is circuit has a T-order of 3, while the synthesis of equation (58a) only contains products of order 2 implying a T-order of 2. We therefore successfully lowered the T-order by 1 at the cost of $\frac{2}{3}$ qubit overhead per truth table column. Larger synthesis yield much higher gains in the T-order but also much higher qubit overhead and additional CNOT gates when compared to 'pure' phase tolerant Gray synthesis. However we reiterate that pure Gray synthesis is not scalable for arbitrary hardware architectures, demanding these drawbacks for real world applications.

Another point we would like to highlight is that the resulting sub expressions do not have to be synthesized with PPRM but an arbitrary synthesis method. In our implementation, we select the method of lowest CNOT count from a pool of methods. This pool contained the Gray synthesis and PPRM synthesis implemented in tweedledum, as well as phase tolerant synthesis and a custom version of the PPRM synthesis, where multicontrolled X gates are being outsourced to a phase tolerant algorithm. For each step of the array oracle synthesis, each method from the pool of synthesis options is tested individually and the optimal method is selected by means of the lowest CNOT count. It showed, that either phase tolerant Gray synthesis or the custom phase tolerant supported PPRM synthesis are optimal in many steps of the synthesis process.

While our implementation might not be directly feasible due to its high demand for classical resources, the general idea seems to yield improvements. We therefore leave the search of an advanced common subexpression elimination algorithm specifically tailored for $\mathbb{F}_2$-polynomials as an open research question. Regarding the overhead in quantum resources we note that it is always possible to resubstitute equations back into each other. As this increases the T-order for the expressions in question, it is not directly clear in which cases doing this is viable. Another open question therefore arises for an automatic procedure, which decides whether an intermediate value is worth calculating.

6. Benchmarking

6.1. Comparison of different synthesis methods

In order to provide meaningful data about synthesis performance, we first elaborate on our benchmarking method. We compare our method for synthesizing Grover oracles to the *Qiskit* implementation and algorithms from the synthesis library *tweedledum* [20].

The evaluation task is to synthesize a database circuit U_D equation (4) corresponding to an array of data which is randomly generated. The lengths of these arrays are discretely being increased in increments of powers of two, resulting in a range from 4 to 1024 data entries. We choose the label size k equal to the bit amount of the truth table i.e. $k = \log_2(N)$.

The metrics of interest are the average CNOT count and the average amount of arbitrary unitary rotations contained in the individual circuits. The latter will be denoted as U count from now on and is obtained by decomposing all occurring single-qubit gate instructions into their elementary rotations, that is:

$$U(\theta, \phi, \lambda) = \begin{pmatrix} \cos\frac{\theta}{2} & -e^{i\lambda}\sin\frac{\theta}{2} \\ e^{i\phi}\sin\frac{\theta}{2} & e^{i(\phi+\lambda)}\cos\frac{\theta}{2} \end{pmatrix}. \tag{59}$$

[16] Note that basic PPRM synthesis can also be supported by phase tolerant Gray synthesis by outsourcing the synthesis of the multi-controlled gates to the phase tolerant algorithm.

Table 2. Comparison of average gate counts between our phase tolerant (PT) synthesis and the *Tweedledum* implementation of Gray synthesis.

	Average CNOT count				Average U count			Average T_m count (T-order)		Qubits	
Data size	PT (Gray-code)	PT (HTSP)	Gray	Difference	PT	Gray	Difference	PT	Gray	PT	Gray
4	8	6	6	0.0%	9	12	33.3%	6 (4)	10 (4)	4	4
8	24	19	33	73.7%	23	40	73.9%	23 (5)	38 (5)	6	6
16	64	59	103	74.6%	60	110	83.3%	63 (6)	119 (5)	8	8
32	160	148	280	89.2%	149	279	87.3%	189 (7)	356 (6)	10	10
64	384	365	709	94.9%	363	693	90.9%	547 (8)	1015 (8)	12	12
128	896	861	1713	99.0%	848	1684	98.6%	1399 (9)	2804 (9)	14	14
256	2048	1979	3967	100.5%	1963	3908	99.1%	3636 (10)	7132 (10)	16	16
512	4608	4509	9022	100.1%	4466	8920	99.7%	9019 (11)	18225 (11)	18	18
1024	10240	10116	20126	99.0%	9985	19937	99.7%	22001 (12)	44835 (12)	20	20

Table 3. Average metrics for the CSE-synthesis. The comparisons are described by procentual increases/decreases with respect to the gate counts obtained from the benchmark of our phase tolerant synthesis using HTSP solutions.

Data size	Average metrics							
	CNOT count	Comparison	U count	Comparison	Qubits	Comparison	T_m count (T-order)	Comparison
4	11	83.3%	8	−11%	9	125.0%	4 (2)	−33.3%
8	31	63.2%	24	4%	14	133.3%	16 (2)	−30.4%
16	69	16.9%	63	5%	21	162.5%	41 (2)	−34.9%
32	151	2.0%	150	1%	34	240.0%	100 (2)	−47.1%
64	316	−13.4%	344	−5%	56	366.7%	221 (2)	−59.6%

The duration and amount of the experiments (30 per datasize) are selected as to provide a reasonable understanding regarding the efficiency of the methods under test. Hence, we have kept the sample fairly small and have not followed the path of statistical testing with the goal to show any statistical significance. The measured gate counts are rounded correspondingly to obtain reasonable results. Furthermore, we additionally show the savings in terms of CNOT counts by using the discussed solutions to the Hamming TSP instead of Gray-code in the phase tolerant synthesis. Those savings are more apparent in the case of smaller data sizes and smooth out when considering larger data sets. This does not have an impact on the U counts and the decrease in quantum resources comes of course at the cost of an increase in classical resources. When comparing our results to *tweedledum*'s Gray synthesis implementation, we consider the CNOT counts obtained by the corresponding implementation of phase tolerant synthesis with the results obtained through the Hamming TSP based approach.

As can be seen from table 2, the comparison of both synthesis methods shows that the phase tolerant synthesis performs twice as good in terms of CNOT count when compared to the Gray synthesis implemented in *tweedledum*. This is an impressive result that is confirmed after comparing the U counts for both methods. For a database with 2^n entries, our phase tolerant synthesis as well as the standard Gray synthesis scale linear with the database size, which is an important property with regard to real world use cases. In the context of such real world use cases, it is not enough to look only at the general U counts. Another interesting metric that can be extracted from the elementary single qubit rotations is the number of T_m gates together with the T-order mentioned above. For this, we search for the U_1 rotations from the circuit data and extract the belonging angular parameters. These parameters are then represented in the most efficient sequence of T_m gates. Thus, we can count all T_m gates and compute the T-order corresponding to the largest occurring m for each circuit. The corresponding data for both synthesis methods is shown in table 2.

In the previous section, we addressed the implementation of scalable logic synthesis with the assumption that the number of qubits will likely increase more than gate precision and circuit depth for upcoming quantum hardware. The data above shows a linear increase in the T-order with increasing data size together with rapidly growing T_m counts. With this in mind, we test a last synthesis method using the common sub-expression elimination technique (CSE) as described before in a similar test scenario. The obtained results are depicted in table 3. As the qubit resources now depend on the modified truth tables, additionally an average qubit count is given as well.

We can only see a noticeable decrease in CNOT counts and U counts at a datasize of 64, whereas the qubit resources are several times larger. Since the qubit resources now depend on the modified truth tables

Table 4. Average metrics for the *TruthTableOracle* with the 'basic' and 'noancilla' option. The comparisons are described by procentual increases/decreases with respect to the gate counts obtained from the benchmark of our phase tolerant synthesis using HTSP solutions.

Data size	Average CNOT count				Average U count				Qubits	
	'basic'	Comparison	'noancilla'	Comparison	'basic'	Comparison	'noancilla'	Comparison	'basic'	'noancilla'
4	9	50.0%	12	100.0%	16	77.8%	24	166.7%	4	4
8	63	231.6%	84	342.1%	113	391.3%	124	439.1%	7	6
16	292	394.9%	420	611.9%	597	895.0%	786	1210.0%	10	8
32	960	548.6%	2722	1739.2%	1993	1237.6%	3551	2283.2%	13	10
64	2590	609.6%	13803	3681.6%	5354	1374.9%	15144	4071.9%	16	12

and hence underlie some degree of variation, we have given the average results. For smaller data sizes, the U counts are roughly on the same level as in the non CSE-supported synthesis methods and the CNOT counts have slightly increased in most of the analyzed cases. The main motivation for implementing the CSE method was to decrease the T-order and T_m counts, which has proven to be highly successful as the T-order was kept constantly at 2 and the T_m counts were reduced by up to 33%. Indeed, we traded a decrease in gate complexity through fewer and considerably less fine phase gates at the cost of an increase in the qubit count and classical resources[17] for potential benefits in real-word applications.

6.2. Comparison with Qiskits TruthtableOracle

As a comparison of the complexity of arbitrary synthesized Grover oracles, we next check our *phase tolerant Gray synthesis* method against the *TruthtableOracle* class implemented in Qiskit Aqua[18]. A brief description of this method can be seen in the official documentation and the source code is publicly available in the corresponding GitHub repository [39].

The Qiskit-synthesized circuits can be further optimized by first minimizing the input truth table via the Quine-McCluskey[19] algorithm [40], in order to find all the essential prime implicants and then by finding the exact cover via employing the DLX[20] algorithm [41]. This is exponentially heavy on classical resources and it turns out that even with those optimizations, there is a huge gap in terms of CNOT counts and U counts. The qubit count can be additionally addressed through a given selection of options concerning the implementation of multi-controlled Toffoli gates, which have a noticeable impact on the CNOT counts and U counts as well. Hence, even when applying those optimizations for the Qiskit methods, we still get the same benchmarking results for the comparison between the different approaches.

We used the same test scenario as for the comparison of the synthesis methods above, however due to memory limitations[21] during the synthesis and optimization process, we have limited the range in data size to a maximum of 64 data entries. The mode for constructing multi-controlled Toffoli gates was first set to the 'basic' setting. The results for the CNOT counts and U counts can be seen in table 4.

The difference in circuit complexity between the *TruthtableOracle* and our method is in significant favour of our method and even more so, when considering the necessary number of qubits for the oracle circuits. The 'basic' option for multi-controlled Toffoli construction delivers the best scaling behavior in terms of gate counts while using $3n - 2$ qubits for the tested data with 2^n entries, as opposed to our method using only $2\,n$ qubits. The option leading to the lowest number of qubits—which is also given by $2\,n$—is the 'noancilla' one. This method leads to a much worse scaling behavior as can be seen in table 4 below.

We also want to mention, that there is another implementation in Qiskit's *PhaseOracle* class, which takes a Boolean expression or a SAT problem in DIMACS CNF format [42] and passes this to the PPRM synthesis method implemented in *tweedledum*. Thus, we do not give a further comparison between our method and the *PhaseOracle* class as we have tested the different synthesis methods implemented in *tweedledum* and identified the Gray synthesis as the most suited method and competitor in the context of array oracle generation for Grover's algorithm.

[17] This means that we are using more qubits and that the computations of the quantum logic synthesis takes longer on the classical computer.

[18] At the time of preparing the current paper, this class is implemented in Qiskit Aqua 0.9.1 but due to a migration mainly to Qiskit Terra this is likely to change in the future.

[19] The Quine-McCluskey procedure is a method for minimizing logical/Boolean formulas based on a standard representation and the identification and elimination of redundant terms.

[20] The DLX algorithm is an approach to solving the **set cover problem** through the methodology of dancing links [41] and was initially developed by Donald Knuth.

[21] We ran the benchmark with a system memory of 32GB.

7. Summary

The current paper provides a first successful attempt for enabling the convenient utilization of Grover's search algorithm capabilities over traditional function/procedure APIs (e.g. *int grover(int [] list_to_search_in, int value_to_search_for)*). The motivation for this research is based on observations in our previous work [14], in which the issues of constructing oracles for Grover database searches was discussed from a user perspective. Indeed, the only way to make quantum computing commercially viable is to provide accessible interfaces for programmers and end users to integrate quantum algorithms in their services and applications.

With regard to Grover's algorithm, such APIs require for the automatic generation of the black box quantum oracles, which contain the database and the element to search for in this database. In this context, our current paper provides a methodology for automatically generating such quantum oracles for arbitrary databases. The generation consists of two main parts: (1) Mapping the database entries to a circuit U_D generated by logic synthesis and (2) tagging the query hash to create the query oracle. The first step is realized through the utilization of beyond state-of-the-art synthesis functions, while the second step can be realized either with the traditional multi-controlled Z gates or with our newly introduced similarity tags. In this regard, one of the main contributions of this paper is given by the phase tolerant enhancement of synthesis procedures, allowing for resource cuts up to 50% within the context of Grover quantum oracle generation. Furthermore, we present a new synthesis method respecting the requirements of scaling the synthesis procedure for real world physical backends.

To summarize: this paper outlines a clear procedure for making the potentials of the powerful quantum algorithm by Grover available to programmers and end users for integration in everyday ICT-systems (e.g. online shops, telecommunication management systems, database search engines, web analytic systems ...). The methodology proposed in this paper generates the belonging quantum oracles automatically, thereby utilizing and leading to innovative methods for quantum logic synthesis. The computational complexity of the methodology is in general higher than the one of classical search. However, our future research works aims at optimizing this complexity through different heuristics, machine learning techniques and optimizations on the proposed approach. By continuously achieving such gradual improvements, one can see a clear path to a full-scale introduction and application of quantum algorithms based on oracles in current development processes and system architectures.

Data availability statement

The data generated and/or analyzed during the current study are not publicly available for legal/ethical reasons but are available from the corresponding author on reasonable request.

ORCID iD

Raphael Seidel https://orcid.org/0000-0003-3560-9556

References

[1] Arute F *et al* 2019 Quantum supremacy using a programmable superconducting processor *Nature* **574** 505–10
[2] Zhong H-S *et al* 2020 Quantum computational advantage using photons *Science* **370** 1460–3
[3] Wu Y *et al* 2021 Strong quantum computational advantage using a superconducting quantum processor (arXiv:2106.14734 [quant-ph])
[4] Zhu Q *et al* 2021 Quantum computational advantage via 60-Qubit 24-Cycle random circuit sampling (arXiv:2109.03494)
[5] Grover L K 1996 A fast quantum mechanical algorithm for database search *Proc. 28th Annual ACM Symp. on Theory of Computing (STOC'96)* (New York: Association for Computing Machinery) pp 212–19
[6] Long G L 2001 Grover algorithm with zero theoretical failure rate *Phys. Rev.* A **64** 022307
[7] Toyama F, van Dijk W and Nogami Y 2013 Quantum search with certainty based on modified Grover algorithms: optimum choice of parameters *Quantum Inf. Process.* **12** 05
[8] Sun G, Su S and Xu M 2014 Quantum algorithm for polynomial root finding problem *2014 10th Int. Conf. on Computational Intelligence and Security* pp 469–73
[9] Gilliam A, Woerner S and Gonciulea C 2021 Grover adaptive search for constrained polynomial binary optimization *Quantum* **5** 428
[10] Chakrabarty I, Khan S and Singh V 2017 Dynamic Grover search: applications in recommendation systems and optimization problems *Quantum Inf. Process.* **16** 153
[11] Baritompa W P, Bulger D W and Wood G R 2005 Grover's quantum algorithm applied to global optimization *SIAM J. Optim.* **15** 1170–84
[12] Borujeni S E, Harikrishnakumar R and Nannapaneni S 2019 Quantum Grover search-based optimization for innovative material discovery *2019 IEEE Int. Conf. on Big Data (Big Data)* pp 4486–9
[13] Brassard G, HØyer P and Tapp A 1998 Quantum cryptanalysis of hash and claw-free functions *Lecture Notes in Computer Science* (Germany: Springer) pp 163–9

[14] Gheorghe-Pop I-D, Tcholtchev N, Ritter T and Hauswirth M 2022 Computer scientist's and programmer's view on quantum algorithms: mapping functions' APIs and inputs to oracles *Intelligent Computing* ed K Arai (Cham: Springer) pp 188–203
[15] Samsonov E, Kiselev F, Shmelev Y, Egorov V, Goncharov R, Santev A, Pervushin B and Gleim A 2020 Modeling two-qubit Grover's algorithm implementation in a linear optical chip *Phys. Scr.* **95** 045102
[16] Mandviwalla A, Ohshiro K and Ji B 2018 Implementing Grover's algorithm on the IBM quantum computers *2018 IEEE Int. Conf. on Big Data (Big Data)* pp 2531–7
[17] Bennett C H, Bernstein E, Brassard G and Vazirani U 1997 Strengths and weaknesses of quantum computing *SIAM J. Comput.* **26** 1510–23
[18] Al-Rabadi A N 2004 *Reversible Logic Synthesis—From Fundamentals to Quantum Computing* vol 1 1st edn (Berlin: Springer)
[19] Criger B, Moussa O and Laflamme R 2012 Quantum error correction with mixed ancilla qubits *Phys. Rev.* A **85** 044302
[20] Schmitt Bruno 2021 tweedledum (available at: https://github.com/boschmitt/tweedledum) (Accessed 27 July 2021)
[21] Meuli G, Soeken M, Roetteler M and De Micheli G 2020 ROS: resource-constrained oracle synthesis for quantum computers *Electronic Proc. Theor. Comput. Sci.* **318** 119–30
[22] Soeken M, Roetteler M, Wiebe N and Micheli G D 2017 Logic synthesis for quantum computing (arXiv:1706.02721 [quant-ph])
[23] Meuli G, Soeken M, Roetteler M, Bjorner N and Micheli G D 2019 Reversible pebbling game for quantum memory management (arXiv:1904.02121 [quant-ph])
[24] 2021 Qiskit TruthTableOracle (available at: https://qiskit.org/documentation/stubs/qiskit.aqua.components.oracles.TruthTableOracle.html) (Accessed 27 July 2021)
[25] 2021 Q# OracleSynthesis (available at: https://github.com/microsoft/Quantum/blob/main/samples/algorithms/oracle-synthesis/OracleSynthesis.qs) (Accessed 27 July 2021)
[26] Anis M S *et al* 2021 Qiskit: an open-source framework for quantum computing (https://doi.org/10.5281/zenodo.2573505)
[27] Chen G, Fulling S A and Scully M O 1999 Grover's algorithm for multiobject search in quantum computing (arXiv:quant-ph/9909040)
[28] Brassard G, HØyer P and Tapp A 1998 Quantum counting *Lecture Notes in Computer Science* (Germany: Springer) pp 820–31
[29] Fino B J and Algazi V R 1976 Unified matrix treatment of the fast Walsh–Hadamard transform *IEEE Trans. Comput.* **C-25** 1142–6
[30] Porwik P 2002 Efficient calculation of the Reed–Muller form by means of the Walsh transform *Int. J. Appl. Math. Comput. Sci.* **12** 571–9
[31] Kebschull U, Schubert E and Rosenstiel W 1992 Multilevel logic synthesis based on functional decision diagrams *[1992] Proc. European Conf. on Design Automation* pp 43–47
[32] Abdollahi A, Saeedi M and Pedram M 2013 Reversible logic synthesis by quantum rotation gates (arXiv:1302.5382 [cs.ET])
[33] Amy M, Azimzadeh P and Mosca M 2018 On the controlled-NOT complexity of controlled-NOT–phase circuits *Quantum Sci. Technol.* **4** 015002
[34] Kunz H O 1979 On the equivalence between one-dimensional discrete Walsh-Hadamard and multidimensional discrete Fourier transforms *IEEE Trans. Comput.* **C-28** 267–8
[35] Miller C E, Tucker A W and Zemlin R A 1960 Integer programming formulation of traveling salesman problems *J. ACM* **7** 326–9
[36] Bhat G and Savage C 1996 Balanced gray codes *Electron. J. Comb.* **3** R25
[37] McKay D C, Wood C J, Sheldon S, Chow J M and Gambetta J M 2017 Efficient *Z* gates for quantum computing *Phys. Rev.* A **96** 022330
[38] Zeng B, Cross A and Chuang I L 2007 Transversality versus universality for additive quantum codes (arXiv:0706.1382 [quant-ph])
[39] 2021 Qiskit Aqua (available at: https://github.com/Qiskit/qiskit-aqua) (Accessed 19 August 2021)
[40] Jain T K, Kushwaha D S and Misra A K 2008 Optimization of the Quine-McCluskey method for the minimization of the Boolean expressions *4th Int. Conf. on Autonomic and Autonomous Systems (ICAS'08)* pp 165–8
[41] Knuth D E 2000 Dancing links (arXiv:cs/0011047 [cs.DS])
[42] 2021 DIMACS CNF format (available at: https://jix.github.io/varisat/manual/0.2.0/formats/dimacs.html) (Accessed 19 August 2021)